Published OnlineFirst April 4, 2017; DOI: 10.1158/1078-0432.CCR-16-1423

Cancer Therapy: Preclinical

Clinical Cancer Research

Characterization of an Immunogenic Mutation in a Patient with Metastatic Triple-Negative Breast Cancer

Yasmine Assadipour[1,2], Nikolaos Zacharakis[1], Jessica S. Crystal[1,3], Todd D. Prickett[1], Jared J. Gartner[1], Robert P.T. Somerville[1], Hui Xu[1], Mary A. Black[1], Li Jia[1], Harshini Chinnasamy[1], Isaac Kriley[1], Lily Lu[1], John R. Wunderlich[1], Zhili Zheng[1], Yong-Chen Lu[1], Paul F. Robbins[1], Steven A. Rosenberg[1], Stephanie L. Goff[1], and Steven A. Feldman[1]

Abstract

Purpose: The administration of autologous tumor-infiltrating lymphocytes (TILs) can mediate durable tumor regressions in patients with melanoma likely based on the recognition of immunogenic somatic mutations expressed by the cancer. There are limited data regarding the immunogenicity of mutations in breast cancer. We sought to identify immunogenic nonsynonymous mutations in a patient with triple-negative breast cancer (TNBC) to identify and isolate mutation-reactive TILs for possible use in adoptive cell transfer.

Experimental Design: A TNBC metastasis was resected for TIL generation and whole-exome sequencing. Tandem minigenes or long 25-mer peptides encoding selected mutations were electroporated or pulsed onto autologous antigen-presenting cells, and reactivity of TIL was screened by upregulation of CD137 and IFNγ ELISPOT. The nature of the T-cell response against a unique nonsynonymous mutation was characterized.

Results: We identified 72 nonsynonymous mutations from the tumor of a patient with TNBC. $CD4^+$ and HLA-DRB1*1501–restricted TILs isolated from this tumor recognized a single mutation in *RBPJ* (recombination signal binding protein for immunoglobulin kappa J region). Analysis of 16 metastatic sites revealed that the mutation was ubiquitously present in all samples.

Conclusions: Breast cancers can express naturally processed and presented unique nonsynonymous mutations that are recognized by a patient's immune system. TILs recognizing these immunogenic mutations can be isolated from a patient's tumor, suggesting that adoptive cell transfer of mutation-reactive TILs could be a viable treatment option for patients with breast cancer. *Clin Cancer Res; 23(15); 4347–53. ©2017 AACR.*

Introduction

Adoptive cell therapy (ACT) using tumor-infiltrating lymphocytes (TILs) has been shown to mediate durable complete responses in patients with metastatic melanoma (1, 2). Recent evidence suggests that tumor regression is mediated by T-cell recognition of unique mutated tumor antigens in melanoma (3–5). Epithelial solid cancers, which make up the vast majority of human malignancies, have far fewer somatic mutations compared with melanoma, and therefore, potentially fewer immunogenic mutations (6). Nine of 10 patients with a variety of gastrointestinal cancers were found to have one to three mutations that gave rise to mutation-reactive T cells. In one patient with cholangiocarcinoma, 26 mutations were identified, one of which, mutated *ERBB2IP*, generated a $CD4^+$ T-cell response capable of mediating an objective tumor response (7, 8). These data demonstrate that a $CD4^+$ T-cell response directed against a single mutated antigen is sufficient to mediate an objective tumor regression.

In the United States, one in eight women will develop invasive breast cancer in their lifetime. Triple-negative breast cancers (TNBCs) are the most aggressive subtype, with higher recurrence, distant metastases, and decreased survival (9). Although TILs have been identified in breast adenocarcinomas by IHC and found to correlate with patient prognosis, little is known about their reactivity or function within the tumor (10, 11). We aim to identify immunogenic mutations in patients with metastatic breast cancer with the ultimate goal of developing an ACT therapy targeting immunogenic mutations for patients with breast cancer.

Materials and Methods

Patient, materials, and cell lines

Tumor 4062 (lung) was resected from a 61-year-old woman diagnosed with metastatic TNBC (NCT00001823). 4062-TILs were generated as described previously (12). Autologous $CD19^+$ B cells were sorted from the patient's apheresis sample

[1]Surgery Branch, NCI, Bethesda, Maryland. [2]George Washington University School of Medicine and Health Sciences, Washington, DC. [3]Robert Wood Johnson Medical School, Newark, New Jersey.

Note: Supplementary data for this article are available at Clinical Cancer Research Online (http://clincancerres.aacrjournals.org/).

Corresponding Author: Steven A. Feldman, Center for Cancer Research, NCI, NIH, 10 Center Drive, Bethesda, MD 20892. Phone: 301-496-4269; Fax: 301-480-4968; E-mail: feldmanst@mail.nih.gov

doi: 10.1158/1078-0432.CCR-16-1423

Published OnlineFirst April 4, 2017; DOI: 10.1158/1078-0432.CCR-16-1423

Translational Relevance

The administration of autologous tumor-infiltrating lymphocytes (TILs) or checkpoint inhibitors can mediate durable tumor regressions in patients with melanoma presumably by targeting immunogenic tumor mutations. However, evidence suggesting that patients with other solid malignancies can benefit from such therapies is limited. We have recently demonstrated that the administration of autologous $CD4^+$ TILs selected for reactivity against a unique somatic mutation can mediate the regression of a metastatic epithelial bile duct cancer. Despite the fact that breast cancers have fewer somatic mutations than melanoma, in this article, we demonstrate that $CD4^+$ TILs recognize a unique somatic mutation in breast cancer. Taken together, these data suggest that adoptive cell transfer of tumor-specific, mutation-reactive TILs is a viable treatment option and could be the basis for a personalized cell therapy for the treatment of patients with breast cancer.

using anti-CD19 microbeads (Miltenyi Biotec) and cultured with irradiated (6,000 rad) NIH-3T3 cells stably expressing CD40L (3T3-CD40L, authenticated by FACS for CD40L) at a 1:1 ratio in B-cell media composed of IMDM media (Life Technologies) supplemented with 10% human serum and 200 U/mL IL4 (Peprotech). Peripheral blood mononuclear cells were cultured in AIM-V medium (Life Technologies) supplemented with 5% human AB serum (Valley Biomedical), 0.05 mmol/L β-mercaptoethanol, 0.1 mmol/L nonessential amino acids, 25 mmol/L HEPES, and 2 mmol/L L-glutamine (Life Technologies). Cells were maintained at 37°C and 5% CO_2. Melanoma cell lines were isolated from surgically resected metastases as described previously (13): mel624 (HLA-$A2^+$/MART-1^+) and mel2963 (HLA-DP^+/MAGE-$A3^+$). These tumor cell lines, authenticated by HLA typing and MART-1 and/or MAGE-A3 expression in the Surgery Branch (SB), were cultured in R10 medium consisting of RPMI1640 (Life Technologies) containing 10% FBS (Hyclone). Partially HLA-DR–matched allogeneic EBV-B cells (authenticated in the SB by HLA typing) were grown in R10 supplemented with 2 mmol/L L-glutamine.

Whole-exome sequencing

Whole-exome sequencing (WES) was performed at Personal Genome Diagnostics (PGDx) and the SB, NCI (Bethesda, MD). A whole-exome library was prepared using Agilent Technologies SureSelectXT Target Enrichment System for paired-end

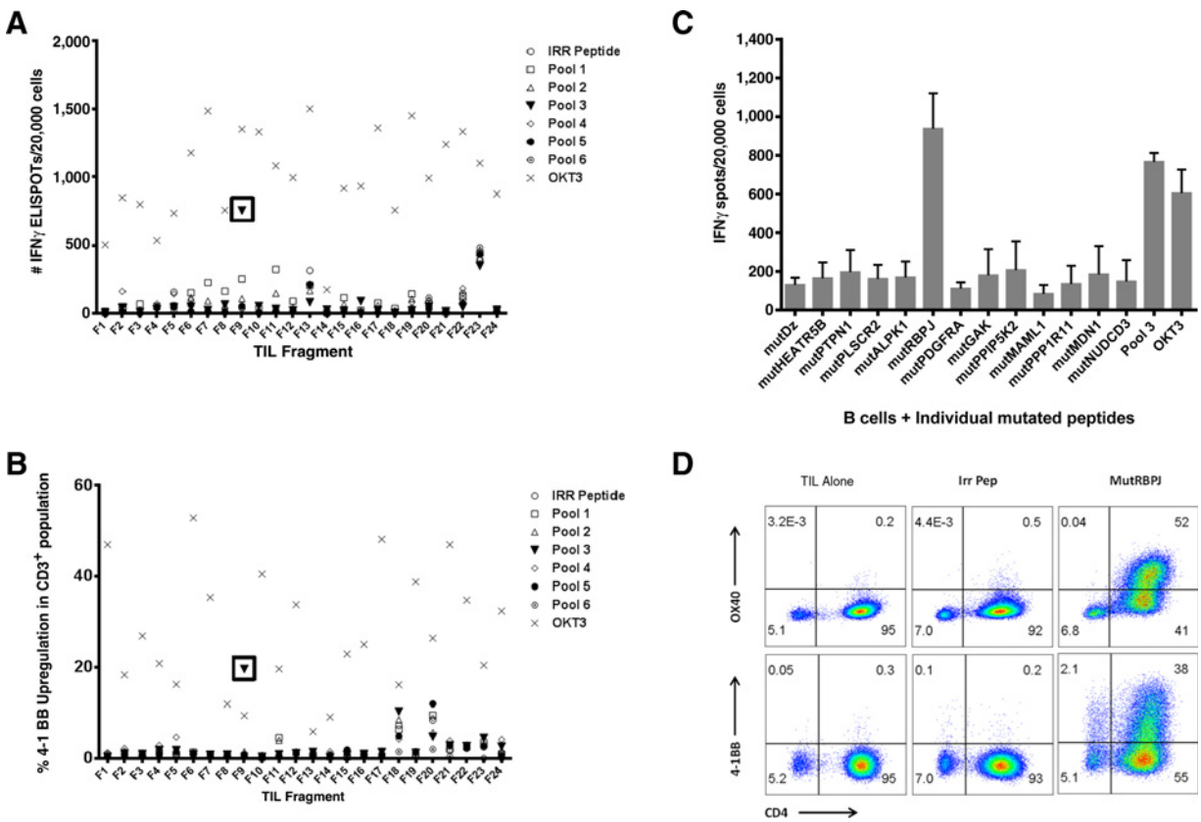

Figure 1.

Identification of an immunogenic mutation recognized by patient 4062-TIL. 4062-TILs were co-cultured with B cells pulsed with the indicated peptide pool (○, irrelevant peptide; □, pool 1; △, pool 2, ▼; pool 3, ◇; pool 4; ●; pool 5; ⊙, pool 6; X, OKT3). **A** and **B,** Twenty-four individual TIL fragments were screened by IFNγ ELISPOT assay (**A**) or upregulation of 4-1BB (**B**) as measured by FACS of cells gated on live $CD3^+$ (box, positive fragment). **C** and **D,** 4062-TILs (F9) were screened against individual peptides comprising peptide pool 3 showing specific recognition of mutated RBPJ by IFNγ ELISPOT (**C**) and specific upregulation of 4-1BB and OX40 in relation to CD4 expression by FACS (**D**). Data are gated on live $CD3^+$ cells.

Published OnlineFirst April 4, 2017; DOI: 10.1158/1078-0432.CCR-16-1423

libraries and sequenced on a NextSeq 500 desktop sequencer (Illumina). The library was prepared using 3-μg genomic DNA (gDNA) isolated from fresh tumor or ten 10-μm OCT sections following the manufacturer's protocol (Agilent Technologies). An mRNA sequencing library was prepared from fresh tumor using Illumina TruSeq RNA Library Prep Kit. In brief, poly(A) mRNA was purified from 1 μg total RNA using oligo-dT magnetic beads and fragmented in the presence of divalent ions at 94°C for 8 minutes. Fragmented RNAs were reverse-transcribed into first-strand cDNAs by random priming, and SuperScriptII followed by second-strand cDNA synthesis. Double-stranded cDNAs were end-repaired, adenylated at the 3′ ends, ligated to indexed sequencing adaptors, and amplified (15 cycles). Paired-end sequencing was carried out on a NextSeq500 sequencer using a mid-output flow cell kit (300 cycles, Illumina). Alignments were performed at SB using Novoalign MPI from Novocraft (http://www.novocraft.com/) to human genome build hg19. Duplicates were marked using Picard's MarkDuplicates tool. Indel realignment and base recalibration was carried out according to the GATK best practices workflow (https://www.broadinstitute.org/gatk/). After cleanup of data, samtools mpileup (http://samtools.sourceforge.net) was used to create pileup files, and Varscan2 (http://varscan.sourceforge.net) was used to call somatic variants. These variants were annotated using Annovar (http://annovar.openbioinformatics.org). We used the following filters to generate putative mutations for evaluation for patient 4062: variant frequency cutoff of $\geq$10% and $\geq$2 variant reads in tumor. Patient 4062 mutations are listed in Supplementary Table S1.

Determination of mutation clustering

4062 WES data were used in the copy-number analysis. The data analysis was performed in the R statistical environment, version 3.3.0. The segmented copy number, cellularity, and ploidy were determined using Sequenza v2.1.2 with normal samples as references and hg19 coordinates. The cancer cell fraction of each mutation was estimated by integrating the local copy number, tumor purity (obtained from Sequenza), and variant allele frequency (VAF). For the given mutations, only mutations with tumor coverage of at least 20× were used. Mutations were defined as clonal if the 95% confidence interval overlapped 1, and subclonal, otherwise (14). All mutations with read depth greater than 3 and VAF greater than 5% were clustered using PyClone v1.3.0 Dirichlet process clustering (15). We ran PyClone with 50,000 iterations and a burn-in of 1,000. In addition, 16 metastases were obtained at autopsy. To detect whether the mutation in recombination signal binding protein for immunoglobulin kappa J region (RBPJ) was present, cDNA was generated from the RNA using Superscript III First-Strand Synthesis System (Life Technologies). gDNA was generated using a DNeasy Kit. *RBPJ*-specific PCR was performed using the following primers: forward 5′CCTCAGCAAGCGGATAAAAG3′ and reverse 3′GCTGTGAACTGGCATGAAAA5′, or forward 5′AGCGAAAGCACTTCATGTTG3′ and reverse 3′GACATGGAGTGGCCTGAAAT5′. Sequencing of PCR products was performed by Macrogen using the first primer set. For genomic DNA samples, *RBPJ*-specific PCR was performed with the primer set forward 5′CCACCTTCTGCTCCAATCAC3′ and reverse 3′TGTAGCCATCTCGGACTGTG5′, followed by sequencing with the same primer set.

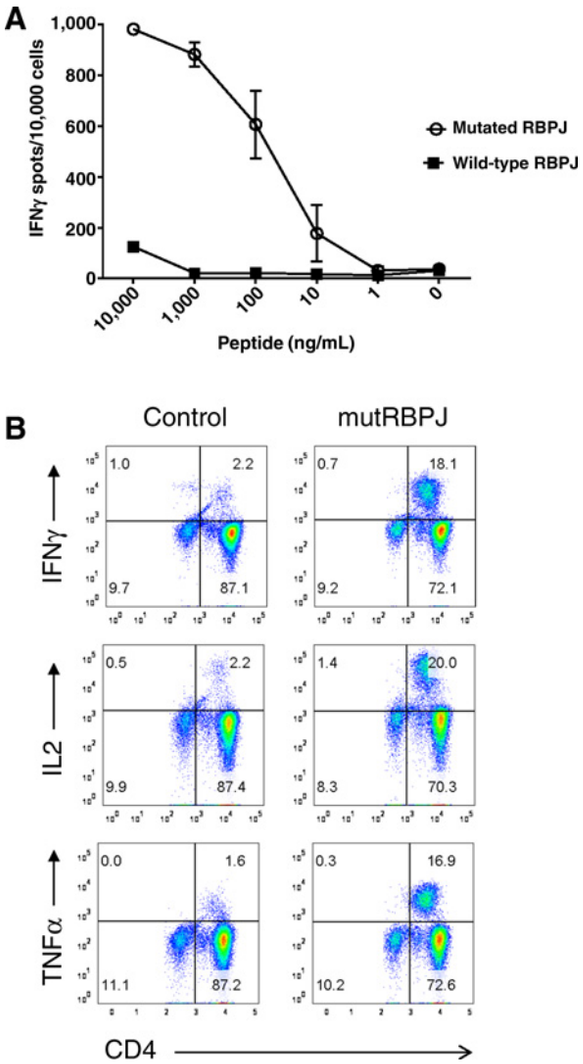

Figure 2.

Specific recognition of RBPJ$^{c.A611T/p.H204L}$ by mutation-specific CD4$^+$ T cells. **A,** Autologous B cells pulsed with 25-mer peptides encoding mutated or wild-type RBPJ were titrated against 4062-TILs (F9). Reactivity against mutated RBPJ using serial dilutions of HPLC-purified mutated and wild-type RBPJ 25-mer peptides was assessed by IFNγ ELISPOT. **B,** Intracellular cytokine staining of mutation-specific RBPJ CD4$^+$ T cells. 4062-TIL (F9) cells were cocultured with autologous B cells pulsed with mutated RBPJ or irrelevant mutated 25-mer peptide identified from another patient with breast cancer (4051, QWKDRAETVIIGDGCVGVSLAYHLA) and stained for CD3$^+$/CD4$^+$/CD8$^+$ then fixed and permeabilized prior to staining for IFNγ, IL2, and TNFα. All data are representative of at least two independent experiments. Error bars, SEM.

Generation of tandem minigenes and peptides

Tandem minigenes were constructed as described previously (7). RNA expression plasmids encoding the minigenes (12 minigenes per TMG) were linearized with the restriction enzyme NsiI. B cells were washed once with PBS and resuspended in Opti-MEM (Life Technologies) at 1.0×10^6 cells/mL. *In vitro* transcribed (IVT) TMG RNA (8 μg) was aliquoted to the bottom of a 2-mm gap electroporation cuvette and 100 μL of B

Published OnlineFirst April 4, 2017; DOI: 10.1158/1078-0432.CCR-16-1423

cells were added. Electroporations were carried out using a BTX-830 square wave electroporator (150 V, 20 ms, 1 pulse). Following electroporation, cells were immediately transferred to polypropylene tubes containing B-cell media, incubated overnight at 37°C, 5% CO_2, and washed once with PBS prior to use in coculture assays.

Individual 25-mer-long long peptides were synthesized (Genscript). Autologous B cells were harvested, washed, resuspended at 1.0×10^6 cells/mL in B-cell media, and incubated with 10 μg/mL individual or pooled peptide overnight at 37°C, 5% CO_2. A mutated peptide from 4051-TIL was used as a negative control (ENSG00000132837, QWKDRAETVIIGDGCVGVSLAYHLA). MHC class II epitope predictions were done using NetMHCIIpan3.1 (www.cbs.dtu.dk/services/NetMHCIIpan/).

Assessment of target cell recognition

TILs were cocultured with peptide-pulsed or electroporated B cells at a 1:5 ratio or with plate-bound OKT3 (1 μg/mL, positive control). Response to targets was measured using an IFNγ enzyme-linked immunospot assay (IFNγ ELISPOT) as described previously (7). Spots were read and quantitated on an Immunospot S6 Microanalyzer (Cellular Technology Limited).

TILs were recovered from the plates and characterized by FACS [CD3-APC-Cy7, CD4-PE, CD8-PE-Cy7, CD134-FITC (OX40), and CD137-APC (4-1BB, BD Biosciences)], and T-cell activation was assessed by upregulation of the activation markers 4-1BB and/or OX40. Finally, TILs were cocultured with autologous EBV-B cells pulsed with peptides in the presence of GolgiStop and GolgiPlug and assessed for intracellular cytokine production according to the manufacturer's protocol (BD Biosciences). TILs were surface stained with CD3-PE-Cy7, CD4-PE prior to fixation and permeabilization, then stained with IFNγ-FITC, IL2-APC, and TNFα-PerCP5.5. FACS was performed on a Canto I instrument (BD Biosciences), and data analysis was performed using FlowJo software (FlowJo LLC).

Assessment of restriction element and minimal epitope

HLA restriction mapping was performed by incubating peptide-pulsed B cells with pan anti-HLA-I W6/32 (Abcam), pan anti-HLA-II IVA12 (SB), anti-HLA-DP (Leinco), anti-HLA-DQ (Beckman Coulter), or anti-HLA-DR (SB) antibodies at 10 μg/1.0×10^5 cells in 100 μL for 2 hours on ice. HLA-DR restriction was confirmed using allogeneic EBV-B cells partially matched at the HLA-DR locus. In an attempt to define the minimal epitope, truncated mutated peptides were synthesized (BioSynthesis) and pulsed onto autologous EBV-B cells at 10 μg/mL. T-cell avidity was assessed by peptide titration using EBV-B cells pulsed with serial dilutions of mutated or wild-type peptide (1–10,000 ng/mL). TIL recognition was assessed by coculture and IFNγ ELISPOT.

T-cell receptor identification

MutRBPJ-stimulated 4062-TILs (F9) were sorted on the basis of expression of $CD3^+$, $CD4^+$, and $4\text{-}1BB^+$ using a FacsJazz Cell Sorter (BD Biosciences). T-cell receptor (TCR) deep sequencing was performed on the sorted cells by Adaptive Biotechnologies. Four TCRs were synthesized (Genscript) using combinations of the two most dominant alpha and beta sequences based on CDR3 frequency. Alternatively, $4\text{-}1BB^+$–sorted cells were subjected to single-cell RNA sequencing (RNA-seq) on the Fluidigm C1, according to the manufacturer's protocol and paired TCR-alpha and beta sequences were identified and synthesized (Genscript). Synthesized TCRs were

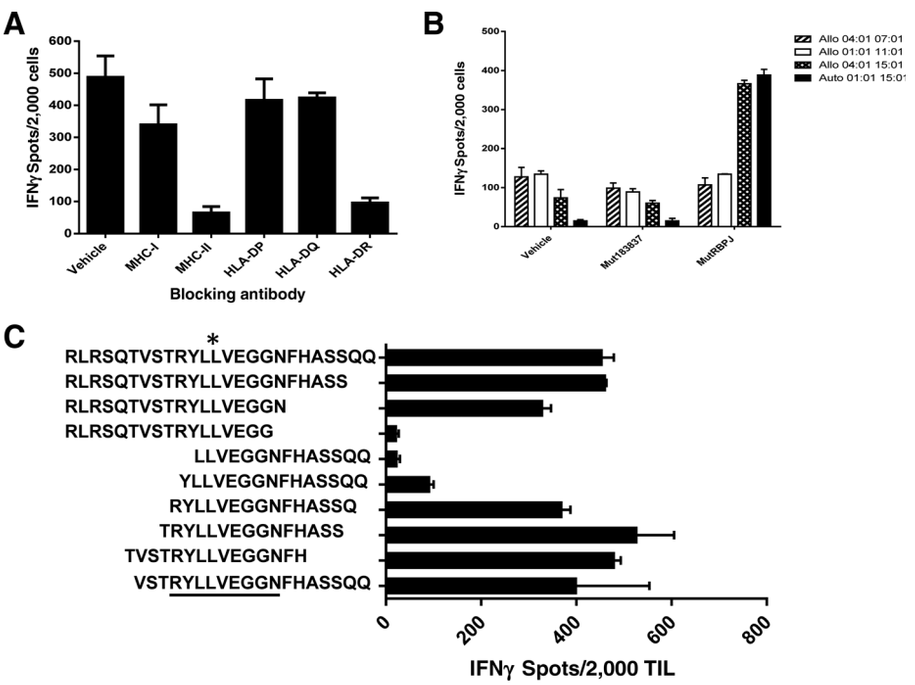

Figure 3.
Characterization of $RBPJ^{c.A611T/p.H204L}$ mutation–reactive T-cell response. 4062-TILs were cocultured with $RBPJ^{c.A611T/p.H204L}$ 25-mer peptide-pulsed autologous B cells that were preincubated with vehicle or the indicated HLA-blocking antibody. **A,** HLA-blocking assay demonstrating MHC class II and HLA-DR restriction. **B,** The HLA-DR restriction element was identified by coculturing 4062-TILs with autologous EBV-B cells or allogeneic EBV-B cells partially matched at the HLA-DR locus. The 4062-TILs $CD4^+$ T-cell response was shown to be HLA-DRB1*15:01 restricted. **C,** 4062-TILs were cocultured with autologous B cells pulsed with $RBPJ^{c.A611T/p.H204L}$ 25-mer peptide or the indicated truncated peptides. *, location of mutated amino acid at position 13, and the predicted peptide binding core sequence is underlined. All data are based on IFNγ ELISPOT and representative of at least three independent experiments. Error bars, SEM.

Published OnlineFirst April 4, 2017; DOI: 10.1158/1078-0432.CCR-16-1423

then cloned into our pMSGV1 gammaretroviral vector backbone for screening.

Results

Patient 4062, a patient with metastatic TNBC, had a lung metastasis resected, and 72 nonsynonymous point mutations were identified after WES of the lesion, 43 of which were expressed on the basis of RNA-seq data (Supplementary Table S1). 4062-TILs were predominantly $CD4^+$ T cells, ranging from 66%–94% (Supplementary Table S2). 4062-TILs were screened and ELISPOT reactivity observed in fragment 9 (F9; 756, PP3 vs. 37, irrelevant peptide) from 4062-TILs to a mutated antigen present in PP3 (Fig. 1A) as well as upregulation of 4-1BB (19.6%, PP3 vs. 0.53%, irrelevant peptide) in the $CD4^+$ T-cell population (Fig. 1B). Similar findings were observed following coculture of 4062-TILs (F9) with B cells electroporated with TMG3 mRNA, which corresponds to the same mutated peptides present in PP3 (Supplementary Fig. S1), suggesting that the exogenous mutated antigen can be

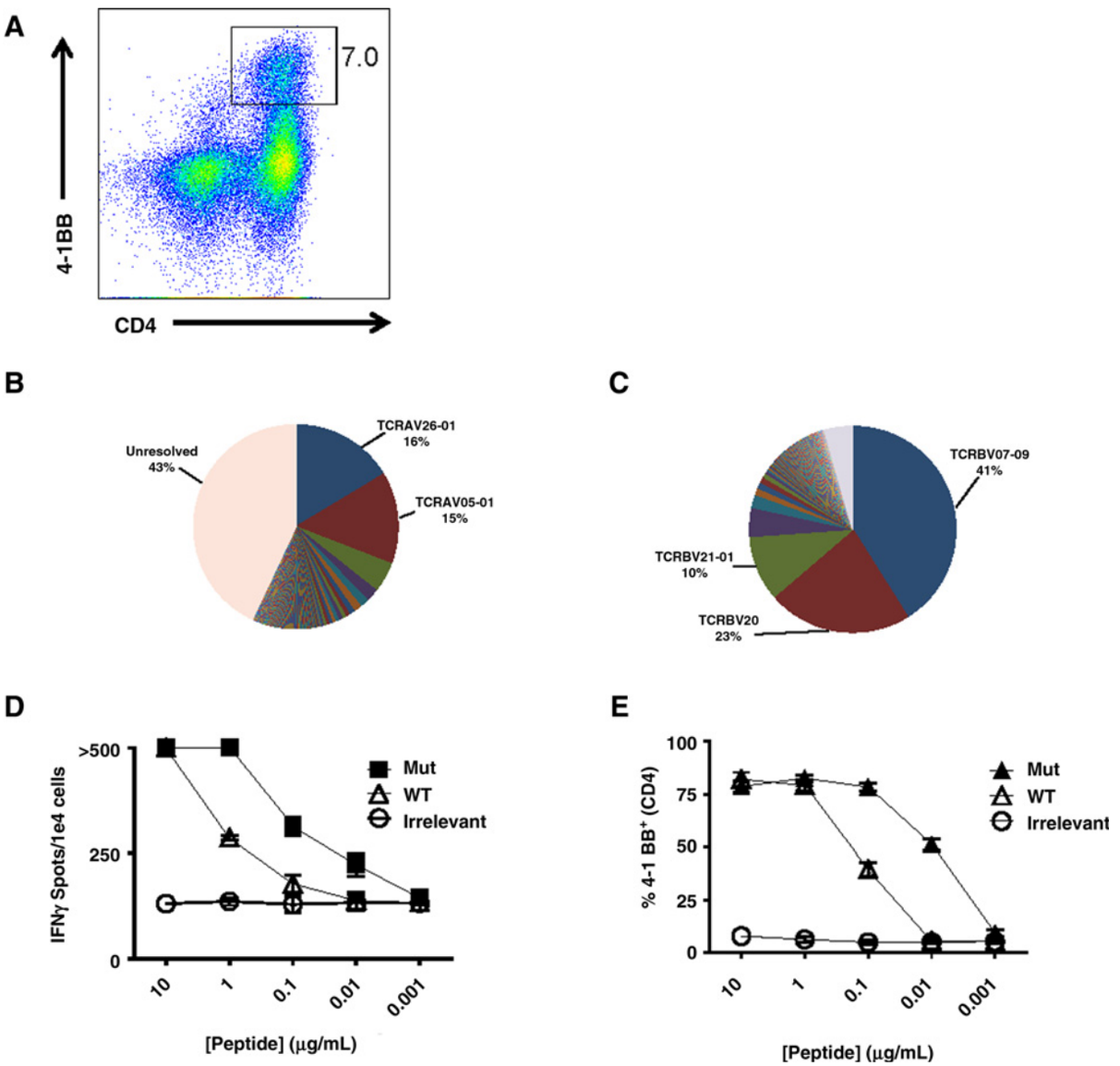

Figure 4.

Identification of RBPJ mutation-reactive TCR. **A,** 4062-TILs were cocultured with autologous APCs presenting $RBPJ^{A611T}$ peptide and sorted on the basis of expression of $CD4^+/4\text{-}1BB^+$ by FACS. Data are gated on live $CD3^+$ cells. **B** and **C,** TCR analysis revealed an oligoclonal population of TCR-α (**B**) and TCR-β (**C**) chains. Of note, 42.9% of the TCR-α chains were unresolved. On the basis of the frequency, the two most frequent TCR-α and TCR-β chains were used to synthesize the four possible TCR combinations. PBL transduced with TCRAV05 (the second most frequent alpha chain) and TCRBV07 (the most frequent beta chain) recognized APCs specifically presenting mutRBPJ based on IFNγ ELISPOT (**D**) and upregulation of 4-1BB (**E**) in the $CD4^+$ T-cell population (▲, mutRBPJ; △, wtRBPJ; ○, irrelevant peptide). Data are representative of three separate patient TCR-transduced PBL.

Published OnlineFirst April 4, 2017; DOI: 10.1158/1078-0432.CCR-16-1423

processed and cross-presented in the context of MHC class II. When screened against the 12 individual peptides in PP3, 4062-TILs (F9) recognized a peptide (RLRSQTVSTRYLLVEGGNFHASSQQ) encoding a mutation in *RBPJ* ($RBPJ^{c.A611T/p.H204L}$) by ELISPOT (Fig. 1C) and upregulation of both 4-1BB and OX40 in the $CD4^+$ T-cell population (Fig. 1D). 4062-TIL (F9) reactivity was specific for $RBPJ^{c.A611T/p.H204L}$ (Fig. 2A) and polyfunctional based on $CD4^+$ T cytokine secretion (IL2, IFNγ, and TNFα, Fig. 2B).

62-TIL (F9) recognition of $RBPJ^{c.A611T/p.H204L}$ was blocked by both a pan anti-MHC class II and anti-HLA-DR antibody (Fig. 3A; Supplementary Fig. S2). HLA-DRB1*1501–restricted based on recognition of allogeneic EBV-B cells partially matched at the HLA-DR locus (Fig. 3B). We identified a core sequence of the potential minimal epitope, RYLLVEGGN (Fig. 3C), suggesting the minimal epitope is likely located within a 15 amino acid sequence, RYLLVEGGNFHASSQ, predicted to be the third highest binding HLA-DRB1*1501 epitope [rank (17%), affinity (257 nmol/L), Fig. 3C]. In an attempt to isolate a reactive TCR, 4062-TILs (F9) were stimulated overnight and the top 7% of the $CD4^+/41BB^+$ T cells were sorted and sent for TCR deep sequencing (Fig. 4A). No dominant TCR clonotype was identified, suggesting that the frequency of the $RBPJ^{A611T}$-reactive cells was extremely low at the time of the sort. Four TCRs containing the two most dominant TCRα [Fig. 4B, TCRAV26 (16.4%) and TCRAV05 (14.5%)] and TCRβ [Fig. 4C, TCRBV20 (41.1%) and TCRVB07 (26.2%)] were synthesized (TCRAV26/TCRBV20, TCRAV26/TCRBV07, TCRAV05/TCRBV20 and TCRAV05/TCRBV07) and cloned into pMSGV1 backbone. Only one low-avidity TCR, TCRAV05/TCRBV07, recognized $RBPJ^{A611T}$ in a dose-dependent manner based on ELISPOT and upregulation of 4-1BB (Fig. 4D and E, respectively). The low T-cell avidity was not based on poor TCR expression, as the TCRAV05/TCRBV07 TCR T-cell transduction efficiency was 70.0% ± 3.2% (range, 63.7%–73.9%, data not shown). In a separate experiment, 4-1BB–sorted T cells were sorted to single cells and analyzed by RNA-seq; however, no additional TCRs reactive against $RBPJ^{A611T}$ were identified (data not shown).

The identification and isolation of mutation-reactive lymphocytes were conducted with the intent to treat patient 4062; however, the patient's disease progressed rapidly, and she expired prior to treatment. At autopsy, the *RBPJ* mutation was detected in all 16 sites of metastases (Supplementary Table S3). We were able to isolate mRNA of sufficient quality for RT-PCR analysis in eight of 16 samples, all of which expressed the mutation at the mRNA level. In addition, analysis of deep sequencing data obtained from the original resected metastasis indicated that 36 of 72 (50%) of the called mutations were clonal, which included $RBPJ^{c.A611T/p.H204L}$, six of 72 (8.3%) were subclonal, and 30 of 72 (41.7%) were unable to be determined due to the number of reads being below the cut-off value (Supplementary Table S1; Supplementary Fig. S3).

Discussion

We demonstrated that TILs isolated from the autologous T-cell repertoire of a patient with TNBC recognized an immunogenic nonsynonymous mutation in RBPJ ($RBPJ^{c.A611T/p.H204L}$). The mutation reactivity was mediated by HLA-DRB1*15:01–restricted $CD4^+$ T cells (Fig. 1). 4062-TIL (F9) reactivity was specific and highly avid against the mutated 25-mer peptide (Fig. 2A) and demonstrated a polyfunctional cytokine profile secreting multiple effector cytokines, including IFNγ, IL2, and TNFα (Fig. 2B). Given the specificity of mutation-reactive 4062-TILs (F9), it was unexpected that we were unable to isolate an avid TCR (Fig. 4). It is likely that the long-term expansion of this culture required to achieve cell numbers sufficient for analysis resulted in a decrease in the frequency of the desired TCR. For TCR gene therapy, the inability to isolate a highly avid TCR points to a potential limitation of this therapeutic approach; however, one could modify the TCR complementarity determining regions (CDRs) to potentially enhance the TCR avidity; however, there are risks associated with such modifications (16).

RBPJ is a ubiquitously expressed nuclear protein that, in the absence of Notch, binds DNA promoter sites and acts as a transcriptional repressor (17, 18). Thus, a mutated RBPJ could potentially dysregulate Notch signaling as a constitutive transcriptional activator or repressor, both of which could play a role in tumor growth. Data suggest the loss of RBPJ function can promote tumorigenesis (19, 20). The functional consequence of an RBPJ mutation ($RBPJ^{c.A611T/p.H204L}$) is not known; however, this mutation was present in all sites of metastasis, and our data suggest that mutated RBPJ is likely a clonal mutation (Supplementary Fig. S3; Supplementary Table S3). Ideally, identification of multiple immunogenic mutations, of both MHC class I and II restriction would likely increase the probability of developing a successful tumor treatment and reduce the need to target clonal mutations. Taken together, these data suggest that there is therapeutic potential for adoptive cell therapy in metastatic breast cancers using mutation-specific TILs.

Disclosure of Potential Conflicts of Interest

No potential conflicts of interest were disclosed.

Authors' Contributions

Conception and design: Y. Assadipour, S.A. Rosenberg, S.L. Goff, S.A. Feldman

Development of methodology: Y. Assadipour, N. Zacharakis, H. Xu, L. Lu, Z. Zheng, Y.-C. Lu, P.F. Robbins, S.L. Goff, S.A. Feldman

Acquisition of data (provided animals, acquired and managed patients, provided facilities, etc.): Y. Assadipour, J.S. Crystal, T.D. Prickett, R.P.T. Somerville, M.A. Black, H. Chinnasamy, I. Kriley, L. Lu, S.L. Goff, S.A. Feldman

Analysis and interpretation of data (e.g., statistical analysis, biostatistics, computational analysis): Y. Assadipour, N. Zacharakis, J.S. Crystal, J.J. Gartner, L. Jia, L. Lu, P.F. Robbins, S.A. Rosenberg, S.L. Goff, S.A. Feldman

Writing, review, and/or revision of the manuscript: Y. Assadipour, N. Zacharakis, J.S. Crystal, T.D. Prickett, J.J. Gartner, I. Kriley, S.A. Rosenberg, S.L. Goff, S.A. Feldman

Administrative, technical, or material support (i.e., reporting or organizing data, constructing databases): J.S. Crystal, H. Xu, M.A. Black, H. Chinnasamy, L. Lu, S.A. Rosenberg, S.L. Goff, S.A. Feldman

Study supervision: S.L. Goff, S.A. Feldman

Acknowledgments

The authors would like to thank Drs. Eric Tran and Alena Gros for technical discussions. In addition, the authors would like to thank Arnold Mixon and Shawn Farid for assistance with flow cytometry.

The costs of publication of this article were defrayed in part by the payment of page charges. This article must therefore be hereby marked *advertisement* in accordance with 18 U.S.C. Section 1734 solely to indicate this fact.

Received June 6, 2016; revised July 11, 2016; accepted March 30, 2017; published OnlineFirst April 4, 2017.

Published OnlineFirst April 4, 2017; DOI: 10.1158/1078-0432.CCR-16-1423

References

1. Dudley ME, Wunderlich JR, Robbins PF, Yang JC, Hwu P, Schwartzentruber DJ, et al. Cancer regression and autoimmunity in patients after clonal repopulation with antitumor lymphocytes. Science 2002;298:850–4.
2. Rosenberg SA, Yang JC, Sherry RM, Kammula US, Hughes MS, Phan GQ, et al. Durable complete responses in heavily pretreated patients with metastatic melanoma using T-cell transfer immunotherapy. Clin Cancer Res 2011;17:4550–7.
3. Lu Y-C, Yao X, Crystal JS, Li YF, El-gamil M, Gross C, et al. Efficient identification of mutated cancer antigens recognized by T cells associated with durable tumor regressions. Clin Cancer Res 2014;20:3401–10.
4. Robbins PF, Lu Y-C, El-Gamil M, Li YF, Gorss C, Gartner J, et al. Mining exomic sequencing data to identify mutated antigens recognized by adoptively transferred tumor-reactive T cells. Nat Med 2013;19:747–52.
5. Monach P, Meredith S, Siegel C, Schreiber H. A unique tumor antigen produced by a single amino acid substitution. Immunity 1995;1:45–59.
6. Alexandrov LB, Nik-Zainal S, Wedge DC, Aparicio SAJR, Behjati S, Biankin AV, et al. Signatures of mutational processes in human cancer. Nature 2013;500:415–21.
7. Tran E, Turcotte S, Gros A, Robbins PF, Lu Y-C, Dudley ME, et al. Cancer immunotherapy based on mutation-specific CD4+ T cells in a patient with epithelial cancer. Science 2014;344:641–5.
8. Tran E, Ahmadzadeh M, Lu Y-C, Gros A, Turcotte S, Robbins PF, et al. Immunogenicity of somatic mutations in human gastrointestinal cancers. Science 2015;350:1387–90.
9. Ismail-Khan R, Bui M. A review of triple-negative breast cancer. Cancer Control 2010;17:173–76.
10. Adams S, Gray RJ, Demaria S, Goldstein L, Perez EA, Shulman LN, et al. Prognostic value of tumor-infiltrating lymphocytes in triple-negative breast cancers from two phase III randomized adjuvant breast cancer trials: ECOG 2197 and ECOG 1199. J Clin Oncol 2014;32:2959–66.
11. Park IH, Kong S-Y, Ro JY, Kwon Y, Kang JH, Mo HJ, et al. Prognostic implications of tumor-infiltrating lymphocytes in association with programmed death ligand 1 expression in early-stage breast cancer. Clin Breast Cancer 2016;16:51–8.
12. Jin J, Sabatino M, Somerville R, Wilson JR, dudley ME, Stoncek DF, et al. Simplified method of the growth of human tumor infiltrating lymphocytes (TIL) in gas-permeable flasks to numbers needed for patient treatment. J Immunother 2012;35:283–92.
13. Topalian S, Solomon D, Rosenberg S. Tumor-specific cytolysis by lymphocytes infiltrating human melanomas. J Immunol 1989;142:3714–25.
14. McGranahan N, Furness AJS, Rosenthal R, Ramskov S, Lyngaa R, Saini SK, et al. Clonal neoantigens elicit T cell immunoreactivity and sensitivity to immune checkpoint blockade. Science 2016;351:1463–9.
15. Roth A, Khattra J, Yap D, Wan A, Laks E, Bilel J, et al. PyClone: statistical inference of clonal population structure in cancer. Nat Meth 2014;11:396–8.
16. Cameron BJ, Gerry AB, Dukes J, Harper JV, Kannan V, Bianchi F, et al. Identification of a Titin-derived HLA-A1–presented peptide as a cross-reactive target for engineered MAGE A3–directed T cells. Sci Transl Med 2013;5:197ra03.
17. High FA, Epstein JA. The multifaceted role of Notch in cardiac development and disease. Nat Rev Genet 2008;9:49–61.
18. Honjo T. The shortest path from the surface to the nucleus: RBP-Jκ/Su(H) transcription factor. Genes Cells 1996;1:1–9.
19. Kulic I, Robertson G, Chang L, Baker JHE, Lockwood WW, Mok W, et al. Loss of the Notch effector RBPJ promotes tumorigenesis. J Expt Med 2015;212:37–52.
20. Tanigaki K, Honjo T. Chapter Seven - Two Opposing Roles of RBP-J in Notch Signaling. In:Raphael K, ed. Current Topics in Developmental Biology: Academic Press; 2010. p. 231–52.

Published OnlineFirst April 4, 2017; DOI: 10.1158/1078-0432.CCR-16-1423

Clinical Cancer Research

Characterization of an Immunogenic Mutation in a Patient with Metastatic Triple-Negative Breast Cancer

Yasmine Assadipour, Nikolaos Zacharakis, Jessica S. Crystal, et al.

Clin Cancer Res 2017;23:4347-4353. Published OnlineFirst April 4, 2017.